(Received 21 November 2024, Accepted 11 February 2025, Scheduled 23 April 2025)

Integrated Generator Design for Double Stator Hybrid Excitation Flux Switching Machine

Nur A. Mostaman[1,*], Erwan Sulaiman[1], Mahyuzie Jenal[1], and Irfan A. Soomro[2]

[1]*Faculty of Electrical Engineering, Universiti Tun Hussein Onn Malaysia, Batu Pahat 86400, Malaysia*
[2]*Department of Electrical Engineering, Quaid-e-Awam University of Science and Technology, Nawabshah, Pakistan*

ABSTRACT: Double Stator Hybrid Excitation Flux Switching Generator (DS-HEFSG) has attracted significant interest in power-generating research owing to its potential for improved performance and sustainability. This research examines the utilization of hybrid excitation to enhance the efficiency of a three-phase DS-HEFSG specifically engineered for low-speed power applications such as renewable energy systems like wind and tidal turbines. The innovative method presents a double stator hybrid configuration for a traditional double stator generator, with performance evaluation performed via 2D finite element simulations. The findings indicate that the DS-HEFSG surpasses traditional topologies, rendering it an optimal selection for this generator configuration. The proposed design significantly increases the 18.76% cogging torque value while the electromotive force increases by approximately 21.62%. The proposed design also decreases permanent magnet eddy-current losses by 24.33%. Enhanced performance is noted in electromagnetic torque, torque ripple, output power, and overall efficiency. These advancements contribute to energy savings and lower maintenance costs, reducing reliance on fossil fuels and supporting the transition to greener energy solutions. The proposed DS-HEFSG with hybrid excitation is a viable alternative for efficient low-speed power production.

1. INTRODUCTION

The growing societal need for energy leads to the depletion of finite resources such as coal, natural gas, and oil. As a result, renewable energy sources like solar power, wind power, and hydropower are considered perpetual means of energy extraction [1]. However, each renewable energy approach has its constraints [2, 3]. To address this challenge, the utilization of distributed generators in distribution networks worldwide is increasing [4, 5]. These generators provide excellent functionality at an affordable cost for consumers while addressing limitations in renewable energy generation.

However, conventional distributed generators in distribution networks require careful consideration of several critical factors. Conventional electric power stations predominantly use synchronous generators (SGs) due to their ability to operate at synchronous speed. These machines require expensive machinery to adjust their speed using a prime mover, often a diesel engine as shown in Figure 1. Additionally, conventional generators, especially SG, face several drawbacks that limit their efficiency and performance in modern applications [6–8]. One of the main challenges is their reliance on brushes and slip rings in the rotor, which leads to higher maintenance requirements and increased wear and tear over time [9].

Furthermore, these generators typically require constant excitation power to maintain the magnetic field, which can result in inefficiency, especially during no-load conditions [10–13]. These limitations highlight the pressing performance at specific speeds, often struggling to adapt efficiently to changing operational demands. Additionally, their mechanical complexity and dependence on rotating components can lead to more frequent breakdowns [14], impacting reliability [15], and raising maintenance costs [16].

To address these challenges, Flux Switching Generator (FSG) has emerged as a promising alternative. Unlike synchronous generators, FSGs significantly improve efficiency and controllability compared to conventional designs [17, 18]. For instance, in 2016, a novel hybrid excited flux bidirectional modulation was introduced by Wang and Niu [19]. The research proved that hybrid excitation machines have improved efficiency and controllability compared to conventional generators. However, the proposed hybrid excitation generator identified challenges related to the stability of the generator, which causes high losses.

Building on these advancements, Zhang et al. investigated the dual stator arrangement and made significant improvements in magnetic flux control and overall system stability [20]. The DS-HEFSG represents a major advance in FSG technology and overcomes many limitations of conventional topologies. The implementation of permanent magnets and field magnets in a

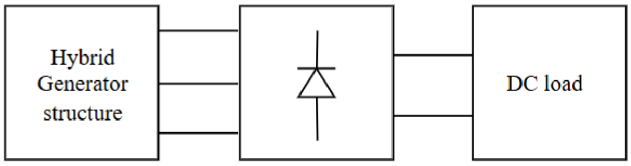

FIGURE 1. Hybrid generator structure.

* Corresponding author: Nur Afiqah Mostaman (afiqahmostaman98@gmail.com).

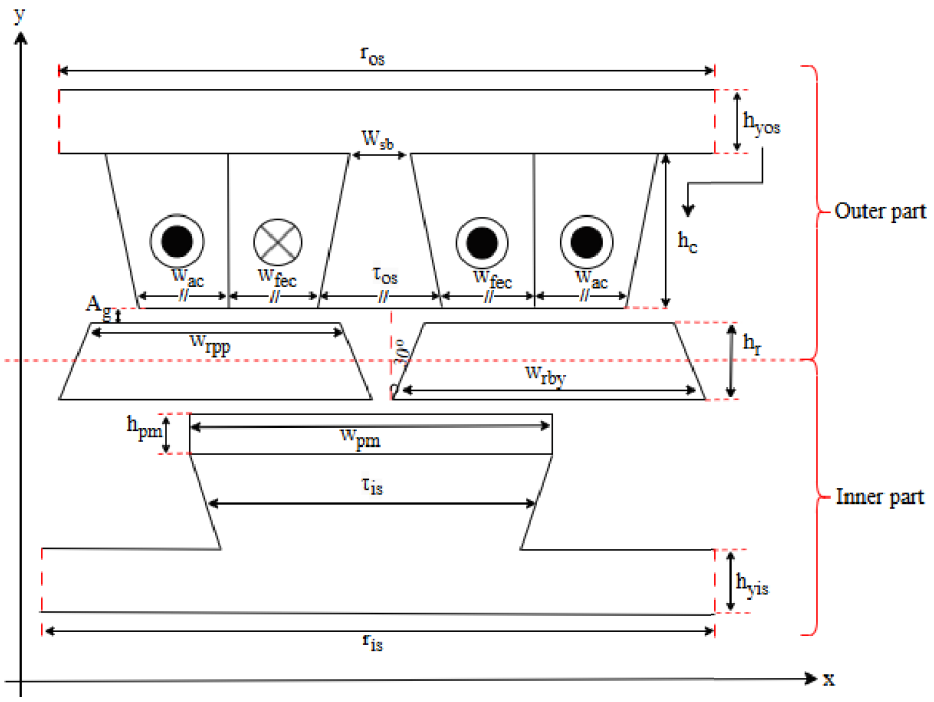

FIGURE 2. Geometrical dimensions of structure.

dual stator configuration enhances magnetic flux regulation and improves system efficiency. However, the designed generator has been identified as not operating under high-speed conditions. By integrating permanent magnets and field windings in the dual stator design by Jan and Mueller, the DS-HEFSG enhances magnetic flux regulation and optimizes performance for low-speed power generation applications [21].

Moreover, DSHE-FSG is an advanced electrical machine that combines permanent magnet and field windings that enhance magnetic flux control, which makes it suitable for optimizing performance in low-speed power generation applications. The hybrid excitation method employed by the DSHE-FSG effectively mitigates the limitations associated with conventional synchronous generators. This approach offers a more resilient and adaptable solution to contemporary power generation requirements, positioning it as a viable option for future implementations. According to their research, they only highlight the optimal performance in terms of dynamic and fault tolerance in the dual stator configurations.

Hence, this paper focuses on the DS-HEFSG and addresses its design principles, operational benefits, and potential applications using the JMAG designer software to overcome flux and voltage regulation problems and reduce generator losses. This research also presents a thorough analysis to emphasize the distinct features of the DS-HEFSG and to illustrate its advantages over conventional generator technologies in multiple practical applications. By examining its design and performance, this study has been compared with conventional generators to explore the potential of DS-HEFSG to revolutionize the field of power generation. This comparison approach minimizes loss generation through enhanced magnetic flux circulation efficiency, adversely affecting the generator's voltage performance.

2. PROPOSED SYSTEM

2.1. Topology Selection for Integrated DS-HEFSG

The design of the DS-HEFSG was approached with the objective of optimizing magnetic flux linkage while minimizing losses to ensure high efficiency. The methodology integrates analytical calculations and numerical simulations to achieve an optimal design. The electromagnetic design is based on fundamental principles such as Maxwell's equations and Faraday's Law, which are applied to calculate key parameters such as magnetic flux density, inductance, and electromotive force (emf) within the stator and rotor. Specifically, the air gap flux density of the generator's performance is calculated using well-established formulas.

Moreover, the proposed DS-HEFSG design aims to minimize magnetic reluctance and maximize flux linkage, enhancing overall efficiency. To achieve this, the stator and rotor core are constructed using silicon steel laminations (35H210) due to their high magnetic permeability and low core loss characteristics. To improve the performance, copper is used for coil because it effectively reduces eddy current and hysteresis losses. Additionally, high-energy-density NdFeB is employed in the permanent magnet. These magnets provide superior magnetic flux density and thermal stability, ensuring reliable operation under varying load conditions. The combination of these materials ensures optimal magnetic performance, reduced power losses, and enhanced efficiency in the DS-HEFSG.

The generator's geometrical dimensions were carefully determined to propose the design, including the stator's outer and inner diameters, rotor diameter, and air gap length as shown in Figure 2. For instance, the stator outer diameter was calculated using a specific formula, ensuring the dimensions aligned with the required output power and efficiency specifications. The

magnetic circuit design incorporates materials selected to minimize magnetic reluctance and maximize flux linkage, with the hybrid excitation mechanism integrating both permanent magnets and field windings to achieve the desired magnetic field distribution.

2.2. Sizing Equation

Sizing equations are crucial in the initial phase of the design process for assessing the preliminary values. Due to the mutual inductance between two windings in AC and field excitation coil (FEC), there must be a coupling relationship between their currents [22]. With consideration of the influence of winding and rotor eccentric displacement on the internal flux linkage of the generator, the d- and q-axis components of the flux linkage for the two winding sets can be obtained from Equation (1) as follows:

$$\begin{bmatrix} \psi_{Md} \\ \psi_{Mq} \\ \psi_{Bd} \\ \psi_{Bq} \end{bmatrix} = \begin{bmatrix} L_{Md} & 0 & M_d x_d & -M_d y_q \\ 0 & L_{Md} & M_q y_d & M_q x_d \\ M_d x_d & M_q y_q & L_B & 0 \\ -M_d y_q & M_q x_d & 0 & L_B \end{bmatrix} \begin{bmatrix} i_{Md}+i_0 \\ i_{Mq} \\ i_{Bd} \\ i_{Bq} \end{bmatrix} \quad (1)$$

where ψ_{Md} and ψ_{Mq} represent the d-axis and q-axis equivalent air gap flux linkages of the torque windings, respectively, while ψ_{Bd} and ψ_{Bq} denote the d-axis and q-axis equivalent air gap flux linkages of the suspension force windings, respectively. Similarly, L_{Md} and L_{Mq} are the d-axis and q-axis self-inductances of the torque windings, and M_d and M_q are the suspension force constants. Parameters x_d and y_q refer to the d-axis and q-axis components of the rotor radial displacement, respectively, whereas i_{Md} and i_{Mq} represent the d-axis and q-axis equivalent control currents of the torque windings. The equivalent excitation current of the permanent magnet, i_0, is defined in the positive direction of the d-axis. Additionally, L_B denotes the self-inductance of the suspension force windings, and i_{Bd} and i_{Bq} are the d-axis and q-axis equivalent control currents of the suspension force windings, respectively.

The primary geometrical values of the generator are set as the target values of specific parameters such as rated power, output voltage, and input current. In the proposed complementary coil design DS-HEFSG, the number of rotor poles (N_r), stator slots (N_s), pole arc ratio (α_{po}), and the number of coil turns are determined using the formulas from the previous design specifications.

$$N_r = N_s \times 1 \pm \frac{k}{2q} \quad k = 1, 2, 3... \quad (2)$$

$$\propto_{po} = \frac{\tau_p}{\tau_m} \quad (3)$$

$$NOT = \frac{\delta_a \times I_a \times \alpha}{J_a} \quad (4)$$

TABLE 1. Design parameters.

Symbol	Parameter (Unit)	Value
r_{os}	Outer stator radius (mm)	142
w_{sb}	Stator back yoke width (mm)	20.0
τ_{os}	Inner stator pole pitch (mm)	41.7
w_{ac}	Armature coil width (mm)	14.1
w_{fec}	Field excitation coil width (mm)	14.1
h_{yos}	Outer stator yoke height (mm)	50.0
h_c	Coil height (mm)	30.5
A_g	Air gap (mm)	1.0
w_{rpp}	Rotor pole pitch width (mm)	39.6
w_{rby}	Rotor back yoke width (mm)	47.4
w_{pm}	Permanent magnet width (mm)	39.6
h_r	Rotor height (mm)	15.0
h_{pm}	Permanent magnet height (mm)	10.1
τ_{is}	Inner stator pole pitch (mm)	27.6
h_{yis}	Inner stator yoke height (mm)	20.3
r_{is}	Inner stator radius (mm)	17.3

where $q = 3$ represents the number of AC phases, and a denotes the area reserved for the repetition of AC winding coil and field excitation coil pairs. The given equations result in inner part constraints of $N_r = 10$ and $t = 1 : 2$. The design parameters outlined in Table 1 were determined through detailed analytical calculations based on the DS-HEFSG design requirements and theoretical considerations. These calculations incorporate key electrical and magnetic principles to optimize the generator's configuration for low-speed applications. Moreover, the appropriate values for all geometrical parameters, illustrated in Figure 1, can be computed as follows.

$$\rho = \frac{\frac{mass}{slot}}{w \times l \times sl} \quad (5)$$

in which ρ represents the material density used for parts such as the permanent magnet. The density of the core material is taken to be 7550 kg/m^3. The variables of w, l, and sl denote the width, length, and stack length of each respective part. These parameters are essential for determining the overall volume and values of the generator components to ensure accurate modeling to achieve high performance.

Moreover, the mathematical modeling for this design was constructed in accordance with Maxwell's equations, which form the foundation for analyzing electromagnetic fields. To examine the theoretical methodology and resolve the partial differential for Maxwell equations, the proposed DS-HEFSG is categorized into five separate parts based on their electromagnetism properties, which are rotor, stator, permanent magnet, armature coil, and field excitation coil. Consequently, this segmentation allows for a precise magnetic flux density at each place. Thus, by treating each part independently, the model can accurately find the complex interactions of the magnetic fields under various conditions [23].

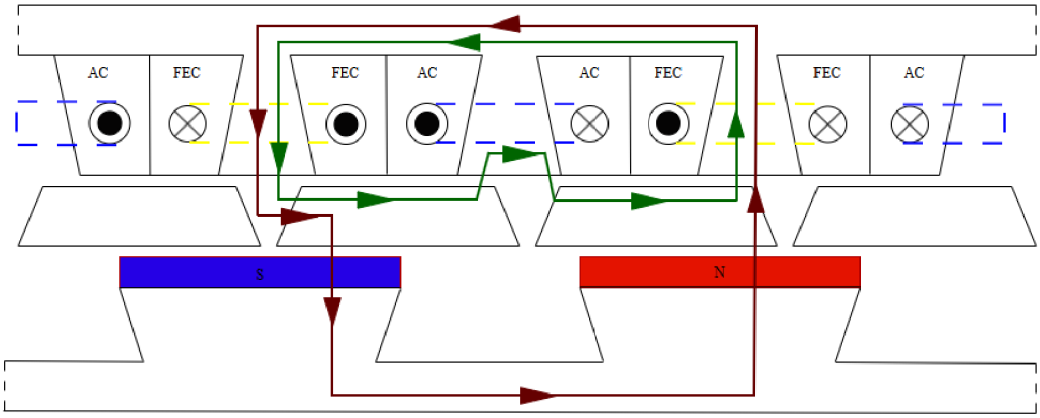

FIGURE 3. DS-HEFSG operational structure.

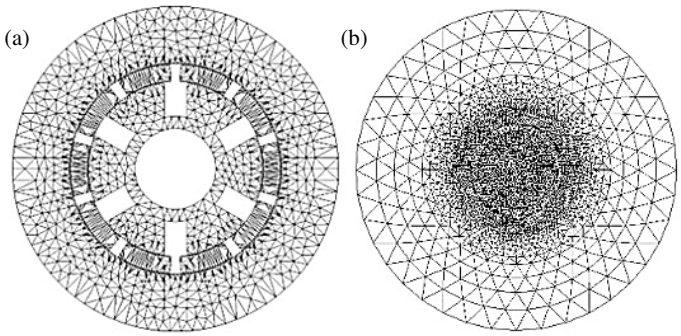

FIGURE 4. Mesh connection of DS-HEFSG. (a) DS-HEFSG. (b) Conventional.

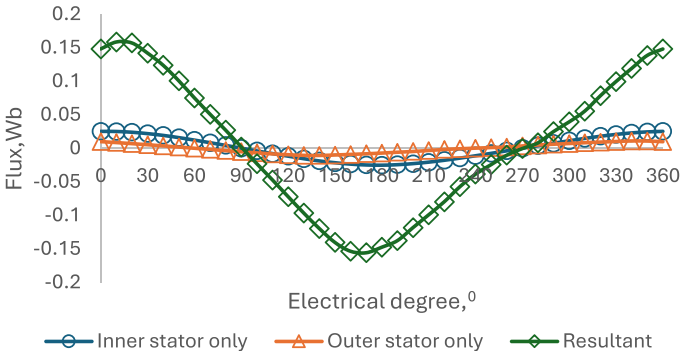

FIGURE 5. Phase coil linkage.

2.3. Working Principles

The operational mechanism of the designed DS-HEFSG can be elucidated either by using Faraday's induction principle or by considering the magnetic circuit. This work adopts a specific methodology to simplify the process. Figure 3 illustrates the linear motion of a single stator pole pitch which represents 360°. The displacement includes two significant points representing positive optimum and negative minimum flux linkage. The red lines represent the flux flow produced by permanent magnets (PMs) and define a series magnetic circuit that includes two stators and a complete mover. The green lines in the flux reflect the contributions of FEC electromagnets, which combine two parallel magnetic circuits and follow PM flux flow pathways. The phase exhibits a positive optimum flux linkage and a negative minimum flux linkage where PM and direct current (DC) electromagnets exhibit similar flux routes, which assure a hybrid excitation theology, bipolar sinusoidal flux coupling, and flux strengthening or weakening characteristics.

3. PERFORMANCE ANALYSIS

3.1. No-Load Conditions

The magnetic circuit configuration of the DS-HEFSG, which operates on the flux switching principle, is significantly more complex than that of conventional radial-field machines. This complexity arises from its unique structure, which integrates axial and radial magnetic flux paths, making the overall magnetic behavior more challenging to predict and analyze. Despite the magnetic field of the DS-HEFSG being uniformly distributed by a single pole pair, the whole field region of the generator, regulated by Dirichlet boundary constraints, requires precise meshing to identify the magnetic fields at various rotor positions precisely. This meshing is essential for accurate computation of electromagnetic properties throughout the generator's operation under no-load conditions. Figure 4 illustrates a two-dimensional finite element method (FEM) model where Figure 4(a) shows the model of the DS-HEFSG, and Figure 4(b) indicates the existing generator, employing a tetrahedral element mesh. The proposed model has over 53,923 mesh elements, offering the requisite complexity for a complex magnetic field dynamics simulation, ensuring the model's precision and dependability in performance forecasts.

In conjunction, the properties of the coil flux linkage under no-load conditions are examined in low-speed values focusing on flux controllability by the field excitation current. Figure 5 presents the differences in peak-to-peak phase flux linkage relative to the electrical degree, emphasizing the outputs from the inner stator and outer stator and their integrated resultant effect. The variation in the RMS phase back-EMF at low speeds demonstrates the response of back-EMF to alterations in rotor speed and field excitation current. This analysis is essential for

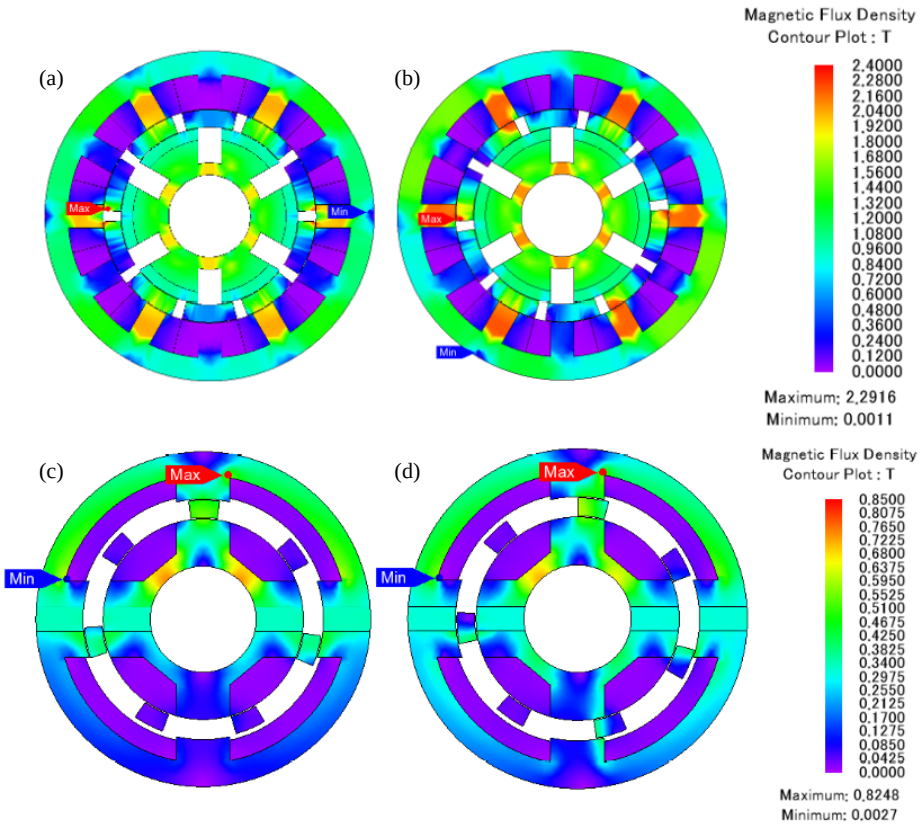

FIGURE 6. Rotor positioned flux distribution, (a) aligned DS-HEFSG, (b) unaligned DS-HEFSG, (c) aligned conventional, (d) unaligned conventional.

comprehending the generator's performance regarding flux regulation and voltage generation across different operational conditions [24].

Additionally, beyond the two specified stators, when the rotor position is within the ranges of 0°–180° or 180°–360°, the maximum value of the vector sum of the phase flux linkages diminishes due to phase discrepancies among the windings. This reduction in the values of the phase flux linkages results in a proportional reduction in the back electromotive force (B-EMF) produced in both sets of armature windings [25]. As the rotor persists in its rotation, the phase flux linkages invert their orientation, thereby completing an average one-pole pitch periodic cycle [26].

Moreover, an illustration of the flux density distribution for aligned and unaligned rotor positions under no-load conditions is shown in Figure 6. The flux density of DS-HEFSG in the back yoke reaches 2.29 Tesla (T) when it is aligned as indicated in Figure 6(a), which means that it stays below the point on the B-H curve of the material that is the lowest while conventional generator only reaches 0.8248 T as shown in Figure 6(c). This proves that the permeabilities of the rotor and stator parts vary with changing operating circumstances and exhibit nonlinear features, hence undermining the accuracy of the analytical model due to magnetic saturation. This indicates that the core operates inside its proportional magnetic domain, prevents magnetic saturation, and ensures that it operates at its most efficient level due to its magnetic properties [27]. To address this, the permeability of the core material necessitates repeated modifications to accommodate saturation effects.

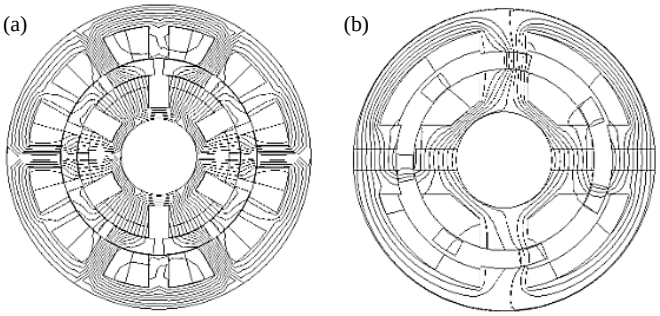

FIGURE 7. Flux line comparison. (a) DS-HEFSG. (b) Conventional.

Furthermore, an additional result comparing the conventional generator and DS-HEFSG is presented in Figure 7 to provide a more comprehensive analysis of the magnetic performance. Flux linkage is a critical parameter that influences the generator's efficiency, output voltage stability, and electromagnetic behavior. The results indicate that the DS-HEFSG exhibits a higher and more uniform flux linkage than the conventional generator. This improvement is attributed to the dual stator configuration and the hybrid excitation method which enhance magnetic flux regulation and minimize leakage.

3.2. Overload Conditions

The generator performance of the proposed DS-HEFSG encompasses a comprehensive evaluation of several important parameters, including output voltage, Total Harmonic Distortion

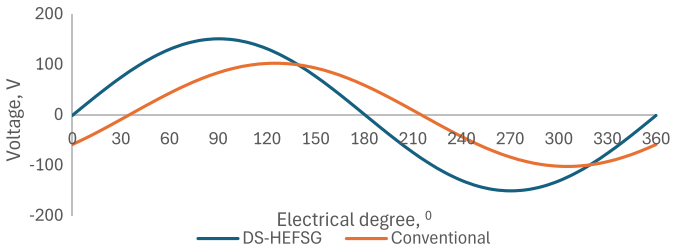

FIGURE 8. Phase voltage.

(THD), cogging torque, field current density, and output power capability under balanced external resistive overload characteristics. The overload condition is specifically designed to assess the generator's robustness and reliability when being subjected to external load demands exceeding the rated operational capacity. A thorough assessment is performed to evaluate the machine's performance under both rated operational conditions and its combined overload capacity.

The majority of studies on PM generators have mainly concentrated on the active component region, namely the PM's location, such as surface-mounted, interior-embedded, or alternatively [16, 28, 29]. This is because PM is the primary and consistent flux source, affecting the distribution of flux lines at synchronous speed. The predominant armature response flux is concentrated within the stator teeth, indicating that the DS-HEFSG may endure irreversible demagnetization of the magnets. Figure 8 depicts the output phase voltage of the three-phase generators functioning at rated circumstances. According to Figure 8, the full-load fundamental phase voltage for DS-HEFSG is 150.86 V, which is approximately higher than the conventional generator voltage, 102.03 V. Furthermore, as illustrated in Figure 9, the generators display symmetrical voltage waveforms characterized by a low total harmonic distortion (THD) spectrum with no torque ripple, resulting from diminished phase EMF harmonics of DS-HEFSG. The minor overshot for DS-HEFSG in the THD waveform is observed in the three-phase, nine-phase, and fifteen-phase generators that results from inadequate distortion, which is attributable to low resistance for both generators.

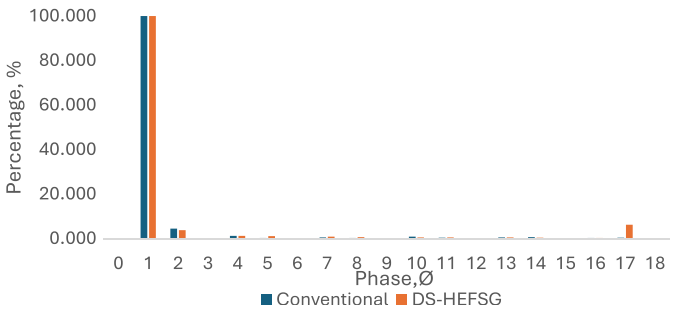

FIGURE 9. THD voltage.

Meanwhile, each magnet functions as a surface-mounted stator, with the rotor teeth integrated into an identical component in the conventional arrangement. In contrast, they are not embedded in the rotor body and maintain an air-gap separation of 1 mm. Hence, a uniform distribution of teeth has led to the

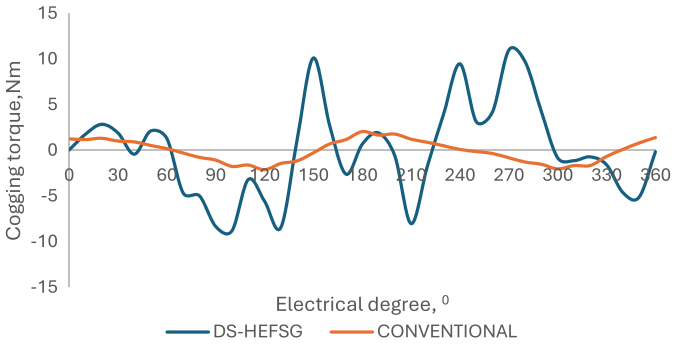

FIGURE 10. Cogging torque of DS-HEFSG.

generator resulting in decreased cogging torque, as indicated in Figure 10, as well as higher harmonic components of EMF. According to the results, despite having various magnetic equivalent circuits, the magnitudes of the air-gap flux densities in the generator's inner and outer stator parts are equivalent. Hence, the cogging torque value for this DS-HEFSG is 10.98 Nm while the conventional generator is 2.06 Nm. This diminutive value arises from the shape of the rotor teeth, the passive rotor configuration, and the circumferentially magnetized permanent magnets within the stator construction [30].

The field current density in a generator plays a crucial role in determining the generator's performance. The field current density of DS-HEFSG is analyzed from 0 Je to 30 Je and is presented in Figure 11. The results demonstrate the capability of the model and the preciseness of the proposed DS-HEFSG. The results of the field's current density are increased to 0 A from 94.17 A. The increase in field current density enhances the magnetic field strength, which leads to higher magnetic flux and consequently increases the electromagnetic force.

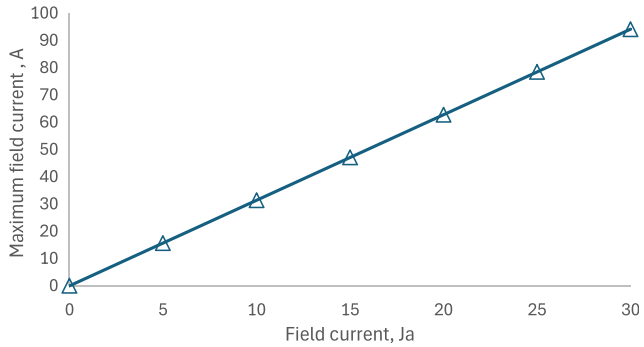

FIGURE 11. Field current of DS-HEFSG.

Moreover, this research then evaluates the generator's capability to sustain consistent operation and efficient power generation under fluctuating load demands to ensure dependability and robustness. This analysis also aims to discover loss processes and optimize efficiency to enhance output performance while assessing voltage control capabilities to ensure that the generator maintains stable voltage levels throughout various operating conditions [31]. The performance data summarized in Table 2 were extracted from the results of JMAG Designer Software as demonstrated in the graphical analyses above. The table describes the generator as being associated

TABLE 2. Performance comparison of generators.

Type of generator	Conventional	Proposed DS-HEFSG
Outer diameter (mm)	284	284
Stack length (mm)	30	30
Flux density (T)	0.8248	2.2916
Back emf (V)	102.03	150.86
Cogging torque (Nm)	2.06	10.98
Field current (A)	-	94.17

with the same dimension, hence the output voltage of the proposed DS-HEFSG is higher than that of the conventional generator. The dual stator parts embedded in the DS-HEFSG lead to an increase in voltage due to low iron losses. This proposed design proved that the arrangement aligns with the simulated self-inductance, which significantly impacts the output parameters of the DS-HEFSG. Consequently, the field's current response has a noble steady-state outcome to the DS-HEFSG.

4. CONCLUSION

In conclusion, this article proposes a novel Double Stator Hybrid Excitation Flux Switching Generator with a surface-mounted permanent magnet. Moreover, the proposed generator has been compared with conventional generators to verify this proposed generator design. The design approach is integrated with 2D finite element method to achieve the optimum configuration of the generator for maximum voltage output. The findings indicate that the DS-HEFSG has substantial power production, elevated induced voltage at lower speeds, and minimal cogging torque. In comparison with the existing conventional generators, DS-HEFSG has below 10% cogging torque value while the conventional generator has 60% cogging torque, although the value of DS-HEFSG is higher than the conventional generator. In addition, DS-HEFSG achieves 21.62% higher electromotive voltage than conventional generators. This investigation also found a significant decrease in PM losses up to 24.33%. This decrease was ascribed to the reduced total harmonic distortion of the air-gap flux density. Consequently, the proposed generator can efficiently satisfy the requirements of low-speed power generation.

Beyond these technical advancements, this research has broader implications for the field of power generation. By demonstrating a design that is more efficient and adaptable to low-speed power generation applications, the DS-HEFSG addresses critical challenges in renewable energy systems. Moreover, the reduction in energy losses and the system's compatibility with renewable energy sources align with global efforts to minimize carbon emissions and transition toward sustainable energy solutions. This study not only advances the understanding of hybrid excitation generators but also paves the way for future research into optimizing magnetic flux circulation and improving generator performances.

ACKNOWLEDGEMENT

This research was supported by the Ministry of Higher Education (MOHE) through the Fundamental Research Grant Scheme (FRGS) (FRGS/1/2023/TK08/UTHM/01/1) and by the Universiti Tun Hussien Onn Malaysia through the Research Enhancement Graduate Grant (RE-GG) VOT (Q082).

REFERENCES

[1] Suhairi, R. C. A., R. N. Firdaus, N. A. M. Zuki, F. Azhar bin Abdul Shukor, M. N. Othman, Z. Ibrahim, and C. Aravind, "Performance characteristics of non-arc double stator permanent magnet generator," *Progress In Electromagnetics Research M*, Vol. 53, 201–214, 2017.

[2] Jaiswal, K. K., C. R. Chowdhury, D. Yadav, R. Verma, S. Dutta, K. S. Jaiswal, K. S. K. Karuppasamy, *et al.*, "Renewable and sustainable clean energy development and impact on social, economic, and environmental health," *Energy Nexus*, Vol. 7, 100118, 2022.

[3] Chau, K.-T., W. Li, and C. H. T. Lee, "Challenges and opportunities of electric machines for renewable energy," *Progress In Electromagnetics Research B*, Vol. 42, 45–74, 2012.

[4] Ufa, R. A., Y. Y. Malkova, V. E. Rudnik, M. V. Andreev, and V. A. Borisov, "A review on distributed generation impacts on electric power system," *International Journal of Hydrogen Energy*, Vol. 47, No. 47, 20 347–20 361, 2022.

[5] Mohammadi, P., H. El-Kishyky, M. Abdel-Akher, and M. Abdel-Salam, "The impacts of distributed generation on fault detection and voltage profile in power distribution networks," in *2014 IEEE International Power Modulator and High Voltage Conference (IPMHVC)*, 191–196, Santa Fe, NM, USA, Jun. 2014.

[6] Mallemaci, V., F. Mandrile, S. Rubino, A. Mazza, E. Carpaneto, and R. Bojoi, "A comprehensive comparison of Virtual Synchronous Generators with focus on virtual inertia and frequency regulation," *Electric Power Systems Research*, Vol. 201, 107516, Dec. 2021.

[7] Liu, J., Y. Miura, and T. Ise, "Comparison of dynamic characteristics between virtual synchronous generator and droop control in inverter-based distributed generators," *IEEE Transactions on Power Electronics*, Vol. 31, No. 5, 3600–3611, 2016.

[8] Mseddi, A., B. Dhouib, M. A. Zdiri, Z. Alaas, O. Naifar, T. Guesmi, B. M. Alshammari, and K. Alqunun, "Exploring the potential of hybrid excitation synchronous generators in wind energy: A comprehensive analysis and overview," *Processes*, Vol. 12, No. 6, 1186, 2024.

[9] Hall, R. D. and R. P. Roberge, "Carbon brush performance on slip rings," in *IEEE Conf. Rec. Annu. Pulp Pap. Ind. Tech. Conf.*, 1–6, San Antonio, TX, USA, Jun. 2010.

[10] Salawu, E. Y., O. O. Awoyemi, O. E. Akerekan, S. A. Afolalu, J. F. Kayode, S. O. Ongbali, I. Airewa, and B. M. Edun, "Impact of maintenance on machine reliability: A review," in *E3S Web of Conferences*, Vol. 430, 1–12, Tamilnadu, India, Nov. 2023.

[11] Odeyar, P., D. B. Apel, R. Hall, B. Zon, and K. Skrzypkowski, "A review of reliability and fault analysis methods for heavy equipment and their components used in mining," *Energies*, Vol. 15, No. 17, 1–27, 2022.

[12] Noland, J. K., M. Giset, and E. F. Alves, "Continuous evolution and modern approaches of excitation systems for synchronous machines," in *2018 XIII International Conference on Electrical Machines (ICEM)*, 104–110, Alexandroupoli, Greece, Sep. 2018.

[13] Tsegaye, S. and K. A. Fante, "Analysis of synchronous machine excitation systems: Comparative study," *International Journal of Energy and Power Engineering*, Vol. 10, No. 12, 1492–1496, 2017.

[14] Das, O., D. B. Das, and D. Birant, "Machine learning for fault analysis in rotating machinery: A comprehensive review," *He-*

liyon, Vol. 9, No. 6, e17584, 2023.

[15] Sheng, C., Z. Li, L. Qin, Z. Guo, and Y. Zhang, "Recent progress on mechanical condition monitoring and fault diagnosis," *Procedia Engineering*, Vol. 15, 142–146, 2011.

[16] Ahamed, R., K. McKee, and I. Howard, "A review of the linear generator type of wave energy converters' power take-off systems," *Sustainability*, Vol. 14, No. 16, 9936, Aug. 2022.

[17] Stephen, D., "Generator performance," *Indep. Gener. Electr. Power*, 1–44, 1994.

[18] Kifune, H., M. K. Zadhe, and H. Sasaki, "Efficiency estimation of synchronous generators for marine applications and verification with shop trial data and real ship operation data," *IEEE Access*, Vol. 8, 195 541–195 550, 2020.

[19] Wang, Q. and S. Niu, "A novel hybrid-excited flux bidirectional modulated machine for electric vehicle propulsion," in *2016 IEEE Vehicle Power and Propulsion Conference (VPPC)*, 1–6, Hangzhou, China, Oct. 2016.

[20] Zhang, Y., Y. Meng, X. Yang, K. Cao, S. Zhang, and Z. Cheng, "Double and triple-vector hybrid modulation model predictive control based on virtual synchronous generator," *Progress In Electromagnetics Research C*, Vol. 148, 43–54, 2024.

[21] Jan, H. U. and M. Mueller, "Design and analysis of dual stator hybrid excited rotary flux switching wave energy generator," in *12th International Conference on Power Electronics, Machines and Drives (PEMD 2023)*, 277–282, Brussels, Belgium, Oct. 2023.

[22] Tarımer, I. and E. O. Yuzer, "Designing of a permanent magnet and directly driven synchronous generator for low speed turbines," *Elektronika Ir Elektrotechnika*, Vol. 6, No. 6, 15–18, 2011.

[23] Tarımer, I. and R. Gurbuz, "Sizing of electrical motors for gearless and directly stimulating applications," *Elektronika Ir Elektrotechnika*, Vol. 84, No. 4, 21–26, 2008.

[24] Sadullaev, N. N., S. N. Nematov, and F. O. Sayliev, "Evaluation of the technical parameters of the generator for efficient electricity generation in low-speed wind and water flows," in *Journal of Physics: Conference Series*, Vol. 2388, No. 1, 012142, 2022.

[25] Tarımer, I. and C. Ocak, "Performance comparision of internal and external rotor structured wind generators mounted from same permanent magnets on same geometry," *Elektronika Ir Elektrotechnika*, Vol. 92, No. 4, 65–70, 2009.

[26] Agrawal, K. C., *Theory, Performance and Constructional Features of Induction Motors*, Ind. Power Eng. Handb., 2001.

[27] Kim, Y. S., "Electromotive force characteristics of current transformer according to the magnetic properties of ferromagnetic core," *Transactions on Electrical and Electronic Materials*, Vol. 16, No. 1, 37–41, 2015.

[28] Aziz, A. A., "Feasibility study on development of a wind turbine energy generation system for community requirements of Pulau Banggi Sabah," Faculty of Mechanical Engineering, Universiti Teknologi Malaysia, Malaysia, 2008.

[29] Stegmann, J. A., "Design and analysis aspects of radial flux air-cored permanent magnet wind generator system for direct battery charging applications," University of Stellenbosch, South Africa, Dec. 2010.

[30] Zhuang, S., G. Liu, and H. Zhu, "Fuzzy dynamic sequential predictive control of outer rotor coreless bearingless permanent magnet synchronous generator based on prediction error compensation," *Progress In Electromagnetics Research C*, Vol. 142, 161–171, 2024.

[31] Huan, J. and H. Zhu, "Design of the outer-rotor coreless bearingless permanent magnet synchronous generator based on an improved MOPSO algorithm," *Progress In Electromagnetics Research M*, Vol. 110, 11–24, 2022.